OPEN

NPG Asia Materials (2013) 5, e77; doi:10.1038/am.2013.70

www.nature.com/am

ORIGINAL ARTICLE

Temperature-controlled directional spreading of water on a surface with high hysteresis

Yongping Hou[1,3], Baolong Xue[1,3], Song Guan[1], Shile Feng[1], Zhi Geng[1], Xin Sui[1], Junhui Lu[1], Longcheng Gao[1] and Lei Jiang[1,2]

The actuation of microscale liquid droplets is a key point in the lab-on-chip field. Marangoni force actuation resulting from a temperature gradient has remarkable advantages. However, high hysteresis between the droplet and the surface is an obstacle to this motion. Here, we take advantage of the temperature-responsive wettability of a surface made of a block copolymer (BCP) to show the temperature-controlled directional spreading of water droplets. By applying a temperature gradient on the BCP surface, both the topologies and chemical components in the nanodomains could be changed gradually. As a result, a wettability gradient force would form with the same direction as the Marangoni force, which could also be formed due to the same temperature gradient, and the collaborative effect of these forces could help overcome the high hysteresis. This was confirmed theoretically by calculating the total force acting on the droplet. The liquid droplet was observed to move by forces of non-mechanical origin in experiments conducted using a thermal gradient on the BCP films. Furthermore, two water droplets were observed to merge into one when they were placed in a V-shaped temperature field. These results help us understand the motion of droplets on a surface with high hysteresis and provide potential applications in microfluidic devices.
NPG Asia Materials (2013) **5,** e77; doi:10.1038/am.2013.70; published online 20 December 2013

Keywords: block copolymer; directional water spreading; PNIPAAm; temperature-controlled

INTRODUCTION

The control of liquid spreading on surfaces has attracted great attention in the fields of painting, printing, DNA microarrays, digital lab-on-a-chip and so on.[1–7] Attaining the control of a liquid as it spreads can be achieved by fabricating groove geometries or patterned surface chemistries to form the wettability gradient. Chu *et al.*[8] harnessed the design of asymmetric nanostructured surfaces to achieve uni-directional liquid spreading, where the liquid propagates in a single preferred direction. Neuhaus *et al.*[9] studied the influence of surface topography and surface functionality on the shape and contact-angle anisotropy of the droplets. Xia *et al.*[10] applied interference lithography to create submicrometer-scale periodic surfaces exhibiting highly anisotropic wetting behavior. Yoshimitsu *et al.*[11] prepared groove structures with large periods and very large heights (on the order of tens to hundreds of micrometers) by wafer dicing. Mele *et al.*[12] demonstrated PDMS (polydimethylsiloxane) stamps of a green leaf, exhibiting an arrangement of periodic microridges separated by interconnected and smooth grooves, appertaining to the vascular system of the plant. Kim *et al.*[13] reported the uni-directional wetting and spreading of a water droplet on stooped polymer nanohairs fabricated by replica molding and oblique electron beam irradiation. In all of these studies, the control of liquid spreading was achieved with wettability gradient force. The preparation of groove geometries or patterned surface chemistries is very complex.

However, directional liquid spreading can also be triggered by thermal Marangoni force using a thermal-gradient surface.[14] Because the surface tension of a liquid/gas decreases with increasing temperature, when a liquid drop contacts the thermal-gradient surface, a corresponding surface tension gradient is also generated. As a result, Marangoni flow is formed.

The thermal Marangoni force is considered to be the driving force that will overcome the viscous drag. If the contact-angle hysteresis (CAH) is low enough, the liquid droplet moves towards the region of low temperatures. However, the liquid motion is hindered by high hysteresis in most cases. The main obstacle to the motion is the CAH. On a surface with high CAH, liquid spreading remains a great challenge. In order to surmount the hysteresis, additional energy, such as vibrational energy,[15] must be supplied to enable the droplet motion. Here, we provide a simple method by combining the

[1]Key Laboratory of Bio-Inspired Smart Interfacial Science and Technology of Ministry of Education, School of Chemistry and Environment, Beihang University, Beijing, People's Republic of China and [2]Beijing National Laboratory for Molecular Sciences (BNLMS), Key Laboratory of Organic Solids, Institute of Chemistry, Chinese Academy of Sciences, Beijing, People's Republic of China
[3]These authors contributed equally to this work.
Correspondence: Professor L Gao, Key Laboratory of Bio-Inspired Smart Interfacial Science and Technology of Ministry of Education, School of Chemistry and Environment, Beihang University, No. 37, Xueyuan Road, Beijing 100191, People's Republic of China.
E-mail: lcgao@buaa.edu.cn
Received 11 August 2013; revised 24 September 2013; accepted 29 September 2013

wettability gradient force and Marangoni force introduced by the same thermal gradient to realize a controllable liquid spreading on a surface with high CAH.

In the present study, the temperature-sensitive surface was formed by self-assembly of a block copolymer (BCP), poly(methyl methacrylate)-*b*-poly(*N*-isopropylacrylamide) (PMMA-b-PNIPAAm), which was hydrophobic at high temperature and hydrophilic at low temperature, as studied previously.[7] By applying a linear variation of temperature on the BCP surface, a nonlinear wettability transition from hydrophobicity to hydrophilicity could be realized. More importantly, the direction of the wettability gradient was the same as that of the Marangoni force. Therefore, cooperation of the wettability gradient force and the Marangoni force could possibly exceed the high hysteresis. Through experimentation and theory, we determined that the spreading features were dependent on the temperature as well as the wettability gradient.

EXPERIMENTAL PROCEDURES

Preparation of the BCP film

The PMMA-b-PNIPAAm (Mn = 46 400, PDI = 1.16) was synthesized by the atom transfer radical polymerization technique following the procedures described in the literature.[7,16] The volume fraction of PNIPAAm in the BCP was 0.55. A BCP film was prepared by the solution-casting method with a 1.0 g ml^{-1} BCP solution in tetrahydrofuran on a glass slide (2 × 2 cm^2) inside a semi-closed box to avoid humidity. After the solvent was slowly evaporated for 24 h, the glass slide was put into an oven at 50 °C for another 24 h and then under vacuum to remove the residual solvent.

Characterization

The CAs of the water droplets were measured by an optical contact-angle meter system (OCA40Micro, Dataphysics Instruments GmbH, Stuttgart, Germany). Two microliters of deionized water was dropped onto the samples (polymer films), and the static and dynamic CAs were measured at least five times via the expansion and shrinkage method, and the average values are reported. To clearly observe the spreading process, BCP film was placed inside a sample chamber. A temperature gradient along the *x* axis was created using a water flow through pipes that ran parallel to an aluminum substrate. The behavior of the spreading process was recorded by the optical contact-angle meter system with a time scale and also with a commercial digital camera (OCA40Micro). Time zero was chosen to be the frame in which the deposited droplets reached an equilibrium shape after they came into contact with the film.

RESULTS AND DISCUSSION

Copolymers containing NIPAAm can be selectively located in the honeycomb structures by a simple water droplet templating method.[17] These pincushion-structured surfaces show thermal-responsive wettability from hydrophobic to superhydrophobic.[18] In contrast to these, the BCP used here self-assembles into a nano-structured lamellar surface and provides temperature-dependent wettability.

In the present study, the temperature-dependent wettability was studied by measuring the static and dynamic CAs for the water droplets at different temperatures (see Figure 1). The static CAs increased from 26° to 93° with an increase in the temperature from 5 to 35 °C, indicating the wettability transition from hydrophilicity to hydrophobicity. The BCP surface has a temperature-dependent wettability because of the cooperation effect of the changes in surface topological structure as well as the hydrogen bonding between NIPAAm and water molecules. According to the former, the *in situ* atomic force microscopic experiments conducted under water at temperatures below and above LCST (lower critical solution temperature) showed changes in both the PNIPAAm conformation and

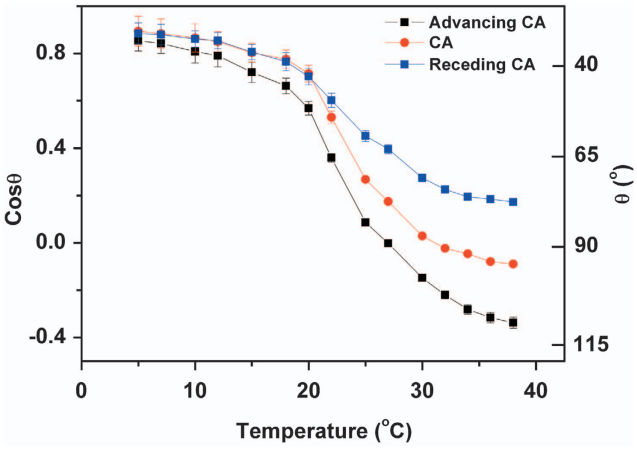

Figure 1 The temperature-dependence of the static CAs of water as well as the advancing and receding CAs for the BCP film are plotted in the form of cosθ versus the temperature, showing a nonlinear wetting behavior of BCP films with increasing temperature.

the PNIPAAm lamellar domains with changing temperature.[7] Below the LCST, PNIPAAm forms inter-molecular hydrogen bonds with the water molecules, leading to a hydrated and swollen state of PNIPAAm. Above the LCST, PNIPAAm forms intra-molecular hydrogen bonds, resulting in a dehydrated and collapsed state. Therefore, the wettability gradient will be formed when a thermal gradient is applied on the surface of the PNIPAAm.

In addition, the advancing and receding CAs also have a similar transition tendency with respect to the thermal gradient. The difference between the advancing and receding angles ($\Delta\theta = \theta_a - \theta_r$) is CAH, which provides the main resistance force.[19–21] In the present work, advancing and receding CA data indicate a contrasting CAH, which provides the main resistance force.[19–21] For instance, the CAH values at 20 and 30 °C were 10° and 14°, respectively. For such high CAH values, the droplet is usually pinned on the surface. Chaudhury and Whitesides[19] stated that the CAH must be less than approximately 10° for drop motion to occur on the wettability-gradient surface. By fitting the current data from Figure 1 into two functions, as shown in Supplementary Figures S1 and S2, the wettability gradient force and the hysteresis force to the water droplet motion can be calculated, which will be discussed later.

A 2-μl droplet of deionized water was placed on a BCP film surface with a 1−dimensional temperature gradient, and the migration behavior was recorded by a charge-coupled device camera. A typical migration behavior of water droplet with a temperature gradient of 2 °C mm^{-1} is shown in Figure 2. Interestingly, the migration behavior was dependent on the initial position of the water droplet in the temperature field. When the temperature at the cold end was 35 °C (hydrophobic region), the droplet was pinned (see Figure 2a). When the temperature was 12 °C (hydrophilic region), the droplet started to spread immediately on the surface, forming a stable wetting state (see Figure 2c). When the water droplet was placed at 25 °C, in the middle transition region, it spread against the temperature gradient and was pinned in the direction perpendicular to the thermal gradient (see Figure 2b). The droplet deposited on the PMMA film surface with the same temperature gradient exhibited no spreading behavior (Supplementary Figure S3). By changing the droplet positions between 12 and 35 °C, we also observed a uni-directional spreading behavior. Therefore, these were the first observations showing a uni-directional spreading behavior of water droplets driven by the forces

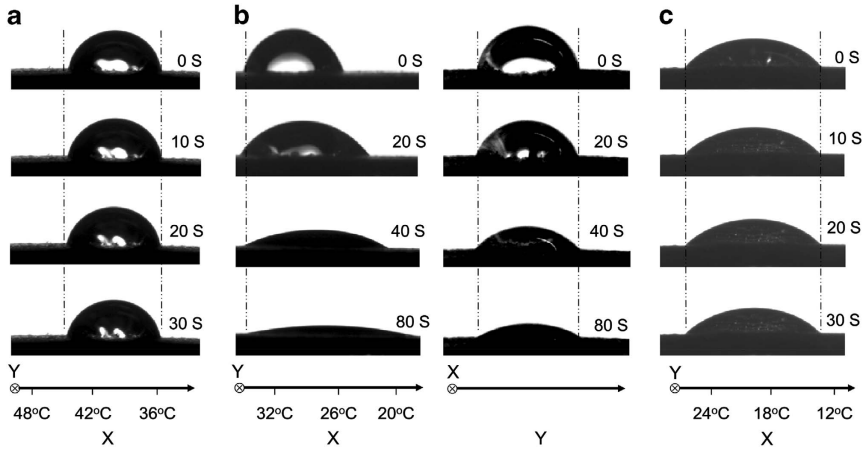

Figure 2 The behavior of water droplet motion on the BCP film with a temperature gradient of 2 °C mm^{-1} at different temperature points: the temperatures at the cold end were (**a**) 35 °C, (**b**) 25 °C, and (**c**) 12 °C. At 12 and 35 °C, the droplet was pinned on the film, while at 25 °C the droplet spread against the temperature gradient and pinned in the direction perpendicular to the thermal gradient, that is, the *y* axis. These results show that the water droplet motion was dependent on the temperature of the position where it was placed.

of non-mechanical origin on a surface with high CAH, although a similar behavior has been observed on other surfaces with a reduced CAH.[22–24]

We applied a V-shaped temperature field on the BCP film (see Figure 3). We dropped two separate water droplets and observed the water droplets spreading toward the cold center, quickly merging into one. This phenomenon can be used as a carrier for chemical reactions in water.

To thoroughly understand the temperature-dependent spreading behavior of water droplets on BCP films, the forces exerted on the water droplets needed to be understood. There are three main forces that influence the motion of droplets: the Marangoni force (F_M), the wettability-gradient force (F_W), and the hysteresis force (F_H).[25]

Brzoska *et al.*[20] first systematically studied Marangoni force induced by a thermal gradient on a silanized silicon wafer. The surface tension of liquid/gas is temperature dependent and decreases as the temperature increases. When the liquid droplet contacts a thermal-gradient surface, the surface tension on the cold side is stronger than on the hot side. The spatial variation in the surface tension results in added tangential stresses, namely, Marangoni force.[26] The Marangoni force is given by

$$F_M = \pi R^2 \frac{d\gamma}{dx} = \pi R^2 \frac{d\gamma}{dT}\frac{dT}{dx} \quad (1)$$

where R is the base radius of the droplet, γ is the surface tension of the water and $d\gamma/dx$ denotes the surface tension gradient, which can be replaced by the product of $d\gamma/dT$ and dT/dx. The value of $d\gamma/dT$ is a constant, and dT/dx is a thermal gradient applied on the surface. The direction of the force is the same as the surface tension gradient, pointing toward the low temperature side.

The most distinguished feature in our system is the nonlinear wettability gradient induced by a temperature gradient. When the water droplet contacts the wettability-gradient surface, the two fronts along the wettability-gradient axis have different CAs. The dynamic CAs of the moving drop are approximately equal to Young's CA in the middle of the droplet base.[27] The wettability-gradient force is described as

$$F_W = \pi R^2 \gamma \frac{d\cos\theta}{dx} = \pi R^2 \gamma \frac{d\cos\theta}{dT}\frac{dT}{dx} \quad (2)$$

where θ is the position-dependent CA. From the data in Figure 1, the values of $d\cos\theta/dT$ at different temperatures could be obtained, and thereby the values of $d\cos\theta/dx$ at different temperature gradient could be obtained. We use the Lorentz and Boltzmann equations to obtain the expression of ($d\cos\theta/dT$) (see Supplementary Materials). The wettability-gradient force has the same direction as the Marangoni force.

Viscous drag, also referred to as the friction force, is opposite to the moving tendency direction of the droplet. Because the viscous drag is typically orders of magnitude smaller than the wettability-driving force,[28] it is not considered here. In actual experimental situations, this resistance force can be calculated from the CAH values.[19–21] The magnitude of the hysteresis force (F_H) is described as[29]

$$F_H = 2R\gamma(\cos\theta_{ro} - \cos\theta_{ao}) \quad (3)$$

where θ_{ro} and θ_{ao} are the position-dependent receding and advancing CAs, respectively. An important consequence of F_H is causing the droplets to adhere to the surface. The data shown in Figure 1 can be used to obtain the values of ($\cos\theta_{ro} - \cos\theta_{ao}$) at different temperatures.

On the basis of the Equations (1), (2) and (3), the total force (F_T) is described as

$$F_T = \pi R^2 \frac{dT}{dx}\left[\frac{d\gamma}{dT} + \gamma\left(\frac{d\cos\theta}{dT}\right)\right] - 2R\gamma(\cos\theta_{ro} - \cos\theta_{ao}) \quad (4)$$

where the first term denotes the driving force due to the wettability-gradient force and Marangoni force and the second term describes the hysteresis force. To demonstrate the extent of variation in the F_T values along the gradient, we chose a representative temperature gradient of 2 °C mm^{-1}. For a given radius of approximately 2.3 mm, the values of F_T as a function of temperature were calculated. The values of F_T initially increase along the temperature gradient, reaching a peak at 25 °C and then decrease to negative values at temperatures above 35 °C. Below 12 °C, the values of F_T are close to zero, and the droplet remains pinned. Above 35 °C, the values of F_T become negative, which indicates that the driving force is far from surmounting the hysteresis force to move the droplet. Therefore, the droplet is pinned on the surface. Between 12 and 35 °C, F_T is large enough, mainly resulting from the temperature-induced wettability gradient, to push the droplet spreading across the thermal gradient.

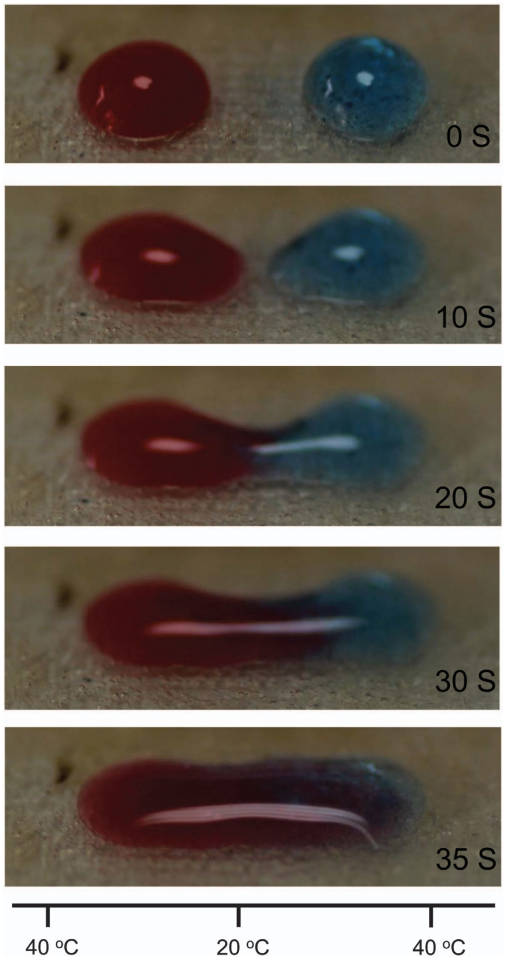

Figure 3 Digital images of opposite-directional spreading of two water droplets (2 μl, colored by red and blue, respectively) on the BCP film in a V-shaped temperature field. Water droplets spread toward to the center and merged into one.

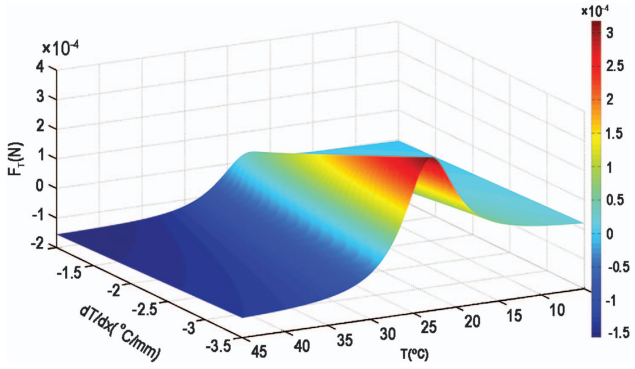

Figure 4 Total force (F_T) calculation exerted on the water droplet versus the temperature (T) and temperature gradient (dT/dx). F_T above zero indicates that the water droplet can spread on the surface, whereas below zero represents the droplet pinned to the surface.

The calculation results are in good agreement with our experimental observations.

Figure 4 shows the F_T values at different temperature gradients and temperatures, exhibiting a hump-like graph. The two regions of the plot are divided by a plane ($F_T = 0$). Points above the plane indicate that when the F_T is above zero, the water droplet should spread, and while below the plane, when the F_T is below zero, the water droplet should be pinned. The experiments carried out at different temperature gradients and temperatures to observe the motion of water droplets were also in accordance with the fitting results. Thus, the motion behavior of the water droplets on a BCP film could be predicted by the values of the temperature gradient and the temperature.

CONCLUSIONS

In conclusion, by taking advantage of the BCP surface with a temperature-responsive wettability, a temperature-controlled directional spreading of liquid was realized in these studies, although the surface had a high hysteresis. The wettability-gradient force and Marangoni force together having the same direction overcame the high hysteresis force and helped the water droplet to move as predicted by the theoretical force calculations. These results could provide potential applications for microfluidic devices.

ACKNOWLEDGEMENTS

We acknowledge the financial support from the National Natural Science Foundation of China (21204002, 51203006), the Specialized Research Fund for the Doctoral Program of Higher Education (20111102120049, 20111102120050) and the National Key Basic Research Program of China (2013CB933000).

1 Chiou, N.-R., Lu, C., Guan, J., Lee, L. J. & Epstein, A. J. Growth and alignment of polyaniline nanofibers with superhydrophobic superhydrophilic and other properties. *Nat. Nano* **2,** 354–357 (2007).
2 Wang, R., Hashimoto, K., Fujishima, A., Chikuni, M., Kojima, E., Kitamura, A., Shimohigoshi, M. & Watanabe, T. Light-induced amphiphilic surfaces. *Nature* **388,** 431–432 (1997).
3 Krupenkin, T. N., Taylor, J. A., Schneider, T. M. & Yang, S. From rolling ball to complete wetting: the dynamic tuning of liquids on nanostructured surfaces. *Langmuir* **20,** 3824–3827 (2004).
4 Hou, Y., Chen, Y., Xue, Y., Wang, L., Zheng, Y. & Jiang, L. Stronger water hanging ability and higher water collection efficiency of bioinspired fiber with multi-gradient and multi-scale spindle knots. *Soft Matter.* **8,** 11236–11239 (2012).
5 Hou, Y., Chen, Y., Xue, Y., Zheng, Y. & Jiang, L. Water collection behavior and hanging ability of bioinspired fiber. *Langmuir* **28,** 4737–4743 (2012).
6 Extrand, C. W., Moon, S. I., Hall, P. & Schmidt, D. Superwetting of structured surfaces. *Langmuir* **23,** 8882–8890 (2007).
7 Xue, B., Gao, L., Hou, Y., Liu, Z. & Jiang, L. Temperature controlled water/oil wettability of a surface fabricated by a block copolymer: application as a dual water/oil on-off switch. *Adv. Mater.* **25,** 273–277 (2013).
8 Chu, K.-H., Xiao, R. & Wang, E. N. Uni-directional liquid spreading on asymmetric nanostructured surfaces. *Nat. Mater.* **9,** 413–417 (2010).
9 Neuhaus, S., Spencer, N. D. & Padeste, C. Anisotropic wetting of microstructured surfaces as a function of surface chemistry. *ACS Appl. Mater. Interfaces* **4,** 123–130 (2012).
10 Xia, D., He, X., Jiang, Y.-B., Lopez, G. P. & Brueck, S. R. J. Tailoring anisotropic wetting properties on submicrometer-scale periodic grooved surfaces. *Langmuir* **26,** 2700–2706 (2010).
11 Yoshimitsu, Z., Nakajima, A., Watanabe, T. & Hashimoto, K. Effects of surface structure on the hydrophobicity and sliding behavior of water droplets. *Langmuir* **18,** 5818–5822 (2002).
12 Mele, E., Girardo, S. & Pisignano, D. Strelitzia reginae leaf as a natural template for anisotropic wetting and superhydrophobicity. *Langmuir* **28,** 5312–5317 (2012).
13 Kim, T.-i. & Suh, K. Y. Unidirectional wetting and spreading on stooped polymer nanohairs. *Soft Matter.* **5,** 4131–4135 (2009).
14 Brochard, F. Motions of droplets on solid-surfaces induced by chemical or thermal-gradients. *Langmuir* **5,** 432–438 (1989).
15 Mettu, S. & Chaudhury, M. K. Motion of drops on a surface induced by thermal gradient and vibration. *Langmuir* **24,** 10833–10837 (2008).
16 Hou, Y., Gao, L., Feng, S., Chen, Y., Xue, Y., Jiang, L. & Zheng, Y. Temperature-triggered directional motion of tiny water droplets on bioinspired fibers in humidity. *Chem. Commun.* **49,** 5253–5255 (2013).
17 Wong, K., Hernández-Guerrero, M., Granville, A., Davis, T., Barner-Kowollik, C. & Stenzel, M. Water-assisted formation of honeycomb structured porous films. *J. Porous Mater.* **13,** 213–223 (2006).

18 Yabu, H., Hirai, Y., Kojima, M. & Shimomura, M. Simple fabrication of honeycomb- and pincushion-structured films containing thermoresponsive polymers and their surface wettability. *Chem. Mater.* **21,** 1787–1789 (2009).
19 Chaudhury, M. K. & Whitesides, G. M. How to make water run uphill. *Science* **256,** 1539–1541 (1992).
20 Brzoska, J. B., Brochard-Wyart, F. & Rondelez, F. Motions of droplets on hydrophobic model surfaces induced by thermal gradients. *Langmuir* **9,** 2220–2224 (1993).
21 Lu, X., Tan, S., Zhao, N., Yang, S. & Xu, J. A unique behavior of water drops induced by low-density polyethylene surface with a sharp wettability transition. *J. Colloid Interf. Sci.* **311,** 186–193 (2007).
22 Chen, J. Z., Troian, S. M., Darhuber, A. A. & Wagner, S. Effect of contact angle hysteresis on thermocapillary droplet actuation. *J. Appl. Phys.* **97,** 014906 (2005).
23 Pratap, V., Moumen, N. & Subramanian, R. S. Thermocapillary motion of a liquid drops on a horizontal solid surface. *Langmuir* **24,** 5185–5193 (2008).
24 Farahi, R. H., Passian, A., Ferrell, T. L. & Thundat, T. Microfluidic manipulation *via* Marangoni forces. *Appl. Phys. Lett.* **85,** 4237–4239 (2004).
25 Bai, H., Tian, X., Zheng, Y., Ju, J., Zhao, Y. & Jiang, L. Direction controlled driving of tiny water drops on bioinspired artificial spider silks. *Adv. Mater.* **22,** 5521–5525 (2010).
26 Nikolov, A. D., Wasan, D. T., Chengara, A., Koczo, K., Policello, G. A. & Kolossvary, I. Superspreading driven by Marangoni flow. *Adv. Colloid Interf. Sci.* **96,** 325–338 (2002).
27 Daniel, S. & Chaudhury, M. K. Rectified motion of liquid drops on gradient surfaces induced by vibrations. *Langmuir* **18,** 3404–3407 (2002).
28 Suda, H. & Yamada, S. Force measurements for the movement of a water drop on a surface with a surface tension gradient. *Langmuir* **19,** 529–531 (2003).
29 Lorenceau, E. & Quéré, D. Drops on a conical wire. *J. Fluid Mech.* **510,** 29–45 (2004).

Supplementary Information accompanies the paper on the NPG Asia Materials website (http://www.nature.com/am)